Inelastic scattering and one-neutron-transfer reactions of $^{18}O+^{40}Ca$

K. E. Rehm, W. Henning, J. R. Erskine,* and D. G. Kovar
Argonne National Laboratory, Argonne, Illinois 60439
(Received 15 March 1982)

Inelastic scattering of $^{18}O+^{40}Ca$ was investigated at $E_{c.m.}=42.85$ MeV in order to study the influence of coupled channels effects. Angular distributions were measured in the angular range $\theta_{lab}=5°-45°$ for elastic scattering and inelastic excitation of the 3^-(3.737 MeV), 2^+(3.905 MeV), 5^-(4.492 MeV) states in ^{40}Ca and the 2^+(1.982 MeV) and 3^-(5.098 MeV) states in ^{18}O. The results are compared to distorted-wave Born approximation and coupled channel calculations employing collective form factors. The improvements of the coupled channel predictions over those of the distorted-wave Born approximation are less dramatic than observed previously for $^{16}O+^{40}Ca$. With the exception of the ground state transition, the spectroscopic factors for the one-neutron-transfer reaction $^{40}Ca(^{18}O, ^{17}O)^{41}Ca$ are in good agreement with those observed in light ion induced reactions.

NUCLEAR REACTIONS $^{40}Ca(^{18}O,^{18}O)^{40}Ca$, $E_{lab}=62.14$ MeV; measured $\sigma(\theta)$; elastic and inelastic scattering; $(^{18}O,^{17}O)$ and $(^{18}O,^{19}F)$ reactions; optical model, DWBA, CC calculations; deduced deformation lengths and spectroscopic factors.

I. INTRODUCTION

With the exception of elastic scattering, inelastic scattering is perhaps the simplest process which can take place during the interaction of two complex nuclei. Owing to the strong absorption occurring in the interaction of heavy nuclei, the analysis of inelastic scattering data is strongly simplified and one-step distorted wave Born approximation (DWBA) calculations have been quite successful in describing a large amount of experimental data. Starting with such good agreement between theory and experiment, one is now able to investigate in detail more complicated multistep processes which require coupled channels (CC) treatments. Several studies have been reported recently[1-5] dealing with heavy ion inelastic scattering reactions which cannot be understood in the framework of simple DWBA calculations. A number of these reactions involve nuclei near closed shells. A well known example[6-8] is the excitation of the 2^+ state in ^{18}O at $E_x=1.982$ MeV. When compared to DWBA calculations the pattern of the experimental angular distribution is found to be shifted to more forward angles by $2°-5°$ and the last maximum of the angular distributions is underpredicted when the usual scaling relation[9] between nuclear and Coulomb deformation length is used in the calculation. A number of explanations have been proposed to explain this behavior, ranging from the inclusion of reorientation effects,[10] and an *ad hoc* change of the nuclear form factor[7,11] to the inclusion of transfer processes.[12] Recently an interpretation has been presented which includes most of the processes mentioned above[13] and which shows that the main contribution comes from the exact treatment of the microscopic nuclear form factor. Similar CC calculations[14] have successfully explained the excitation of ^{17}O in the reaction $^{17}O+^{40}Ca$ at $E_{lab}=61.07$ MeV. In this paper we present results of measurements of inelastic scattering of ^{18}O on ^{40}Ca at $E_{lab}=62.14$ MeV in order to further investigate the projectile excitation behavior of ^{18}O. The $^{18}O+^{40}Ca$ reaction also presents an opportunity to investigate the anomaly observed in the angular distribution for the $^{40}Ca(5^-$ 4.492 MeV) excitation in the $^{16}O+^{40}Ca$ reaction. The laboratory energy chosen corresponds to a center of mass (c.m.) energy identical to that of the previously studied $^{16}O+^{40}Ca$ system. In comparison to the $^{16}O+^{40}Ca$ reaction, more transfer and inelastic channels contribute to the reaction cross section. In particular some of the transfer channels exhibit transition strengths of the same magnitude as inelastic excitations. Therefore, angular distributions for the strongest transfer channels, i.e. $(^{18}O,^{17}O)$, leading to excited states at low excitation energy in ^{41}Ca have also been analyzed.

II. EXPERIMENTAL DETAILS

The experiment was performed with ^{18}O beams at $E_{lab}=62.14$ MeV from the Argonne National Laboratory FN tandem. The scattered particles were momentum analyzed in the Enge split-pole magnetic spectrograph and detected in the focal plane with a position sensitive ionization chamber.[15] Details of the experimental procedure used to obtain the absolute cross section are given in Ref. 3. Because the strengths of transfer channels in ^{18}O induced reactions can be of the same magnitude as those of inelastic scattering, good charge and mass resolution is necessary for extraction of reaction yields, in particular for transitions to states at high excitation energy. Figure 1(a) shows a spectrum of the differential energy loss, ΔE, versus total energy, E_{total}, as measured in the focal plane ionization detector, with the spectrograph set at a scattering angle of $\theta_{lab}=28°$. In the analysis the region for oxygen ions was selected, and the events are displayed in Fig. 1(b) as a function of E_{total} versus magnetic rigidity $B\rho$. The strong transitions to low-lying states in ^{41}Ca populated via the $(^{18}O,^{17}O)$ reaction are clearly observed.

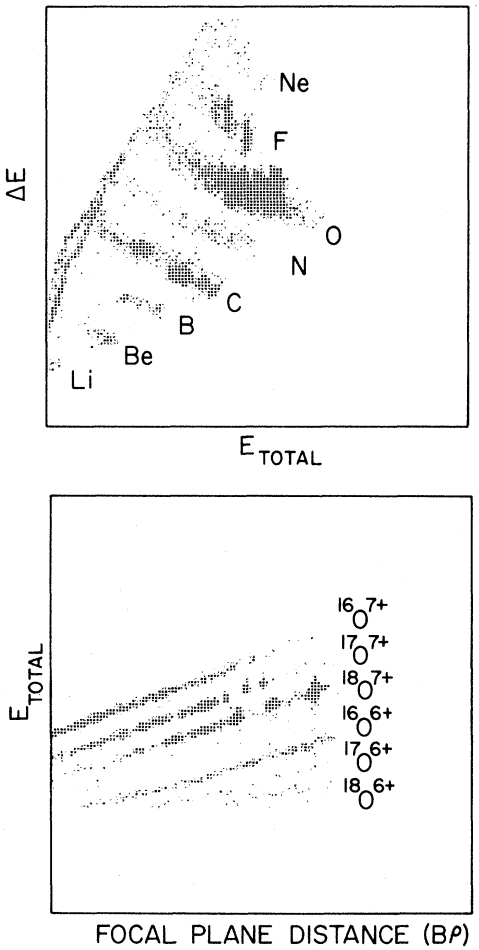

FIG. 1. (a) Differential energy loss, ΔE, versus total energy, E_{total}, and (b) magnetic rigidity, $B\rho$, versus total energy, E_{total}, for the reaction $^{18}O+^{40}Ca$ at $E_{lab}=62.14$ MeV and $\theta_{lab}=28°$.

III. EXPERIMENTAL RESULTS

A. Inelastic scattering

In Fig. 2 an energy spectrum of inelastically scattered ^{18}O particles from ^{40}Ca at $\theta_{lab}=28°$ is compared with that observed for ^{16}O scattering from ^{40}Ca at the same c.m. energy. The ^{18}O spectrum is dominated by the transition to the 1.982 MeV 2^+ state in ^{18}O, which is Doppler broadened due to the γ decay. The structure in the shape observed for the 2^+ state reflects its m-substate population; however, the energy resolution of ≈ 100 keV in the present experiment is not sufficient to extract detailed information about the m-substate population. The 4^+ state in ^{18}O at 3.55 MeV is very weak, while the 3^- state in ^{40}Ca is strongly excited. The 2^+

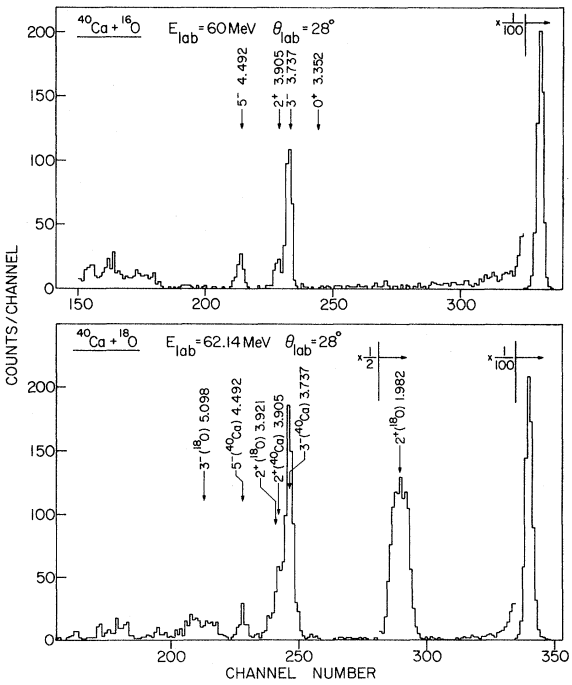

FIG. 2. Energy spectra for elastic and inelastic scattering for the reactions $^{16}O+^{40}Ca$ (top) and $^{18}O+^{40}Ca$ (bottom) at $E_{c.m.}=42.85$ MeV.

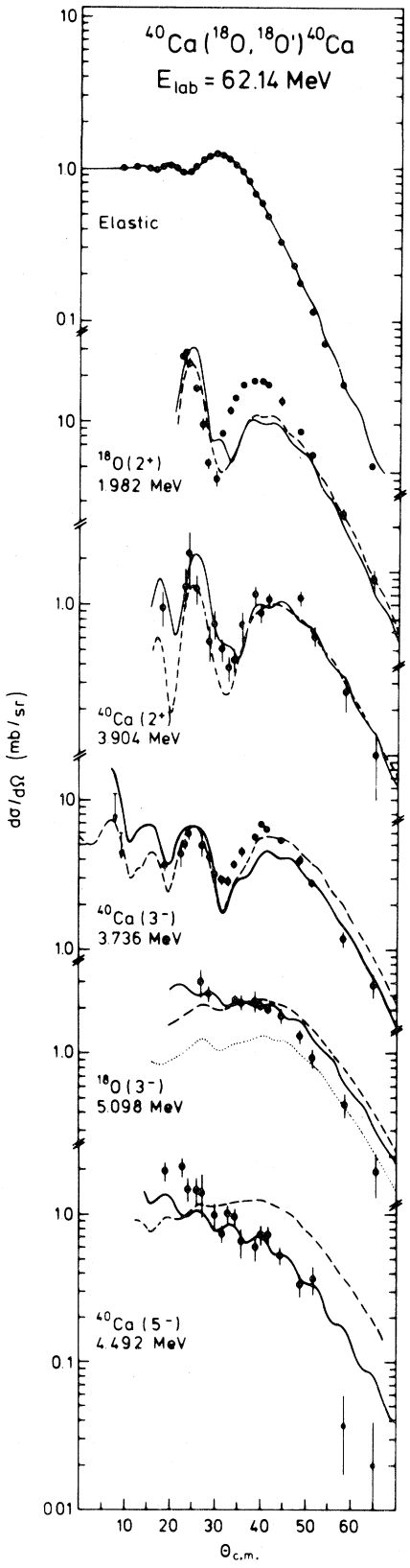

FIG. 3. Angular distributions for elastic and inelastic scattering of $^{18}O+^{40}Ca$ to several states in ^{40}Ca and ^{18}O. The dashed curves are optical model (elastic) and DWBA calculations (inelastic) using the potential given in Table I and the deformation lengths given in Table II. The solid curves are the result of coupled channel calculations as discussed in the text.

state in ^{40}Ca at $E_x=3.905$ MeV is not completely resolved at this angle from the strong 3^- transition due to contributions from the second 2^+ state of ^{18}O at $E_x=3.921$ MeV. The angular distribution shown in Fig. 3 contains contributions from both 2^+ transitions. The 5^- state in ^{40}Ca at $E_x=4.492$ MeV coincides with a 1^- state in ^{18}O at 4.456 MeV; the 1^- state is, however, weakly excited[16] in inelastic scattering of ^{16}O on ^{18}O and should therefore not contribute significantly to the yield observed for the 5^- state. At $E_x\sim5.1$ MeV we observe a broad state which is not present in the corresponding ^{16}O spectrum and is identified as the 3^- state at 5.098 MeV in ^{18}O. This state is strongly excited[17] in $(\alpha\alpha')$ scattering on ^{18}O, and, because of its decay to the 2^+ state at 1.982 MeV by a 3.116 MeV γ ray,[18] should be strongly Doppler broadened. Although the level density becomes too high to resolve individual states at higher excitation energies, the broad peak observed at $E_x=6-7$ MeV in the ^{16}O spectrum is probably the 3^- state of ^{16}O located at 6.13 MeV.

The angular distributions for the elastic scattering and for inelastic excitations of the 2^+ states at $E_x=1.982$ MeV (^{18}O), 3.905 MeV (^{40}Ca), and 3.921 MeV (^{18}O), the 3^- states at $E_x=3.737$ MeV (^{40}Ca) and 5.098 MeV (^{18}O), and the 5^- state at 4.492 MeV (^{40}Ca), are shown in Fig. 3. The dashed lines are DWBA and the solid lines are coupled channels calculations performed with the code PTOLEMY[19] which will be discussed in detail in Sec. IV.

B. Transfer reactions

As can be seen in Fig. 1(a), elements with nuclear charge $Z=3-10$ are observed in the outgoing channels of the reaction $^{18}O+^{40}Ca$. An investigation of the energy spectra reveals that in most cases, e.g., for the reactions (^{18}O,$^{12,13,14}C$), (^{18}O,^{15}N), and (^{18}O,^{16}O), states at high excitation energy are populated in the residual nuclei. In Fig. 4 energy spectra for the reactions (^{18}O,^{17}O) and (^{18}O,^{19}F) are shown where discrete levels close to the ground states are populated with appreciable strength. For the reac-

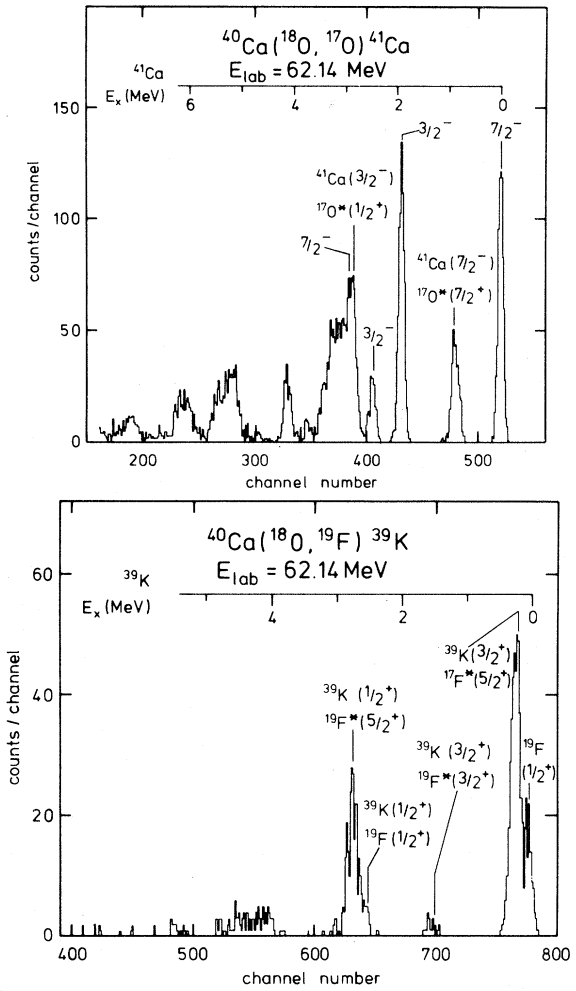

FIG. 4. Energy spectra for the reactions ^{40}Ca(^{18}O,^{17}O)^{41}Ca and ^{40}Ca(^{18}O,^{19}F)^{39}K measured at $\theta_{lab}=27°$ and $\theta_{lab}=28°$, respectively, at an incident energy of 62.14 MeV.

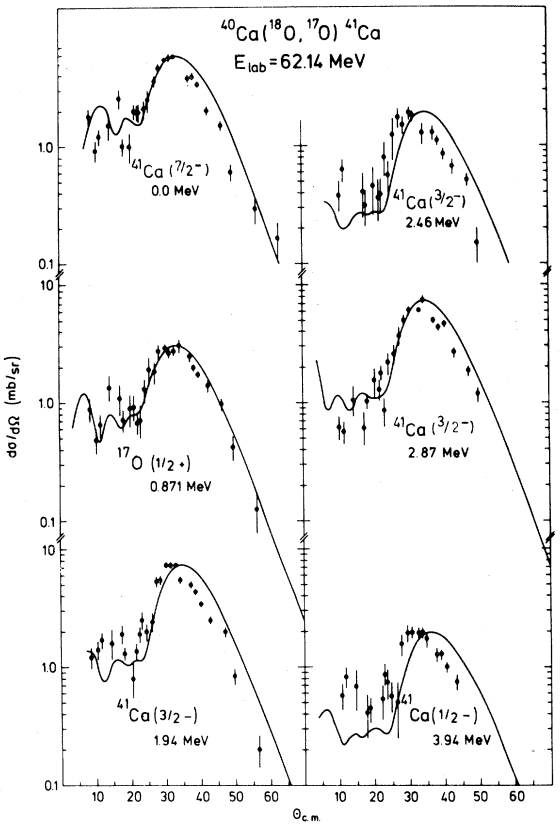

FIG. 5. Angular distributions for the one-neutron transfer reaction ^{40}Ca(^{18}O,^{17}O)^{41}Ca. The solid lines are DWBA calculations with spectroscopic factors given in Table III. For the bound state potential the following parameters were used: $r_0=1.2$ fm, $a=0.65$ fm, $V_{so}=7$ MeV.

tion ^{40}Ca(^{18}O,^{17}O)^{41}Ca low-lying negative parity states in ^{41}Ca at 0.0 MeV ($\frac{7}{2}^-$), 1.943 MeV ($\frac{3}{2}^-$), 2.462 MeV ($\frac{3}{2}^-$), and 3.944 MeV ($\frac{1}{2}^-$) are strongly excited. When compared to the (d,p) reaction,[20,21] it is observed that, in addition, states at $\sim$3.0, 5.0, and 6.0 MeV excitation energy are strongly populated. The strength at around 5 MeV excitation energy might be largely due to the $\frac{9}{2}^+$ state of ^{41}Ca(4.97 MeV). The level density, however, is already so high that a definite identification cannot be made with the present resolution. From Fig. 4 it can be seen that the energy spectrum for the ^{40}Ca(^{18}O,^{17}O)^{41}Ca reaction is complicated due to the excited states of ^{17}O. Thus, the peaks observed at 0.871 and 2.8 MeV excitation energy are associated with ^{17}O in its excited $\frac{1}{2}^+$ (0.871 MeV) state and ^{41}Ca in the $\frac{7}{2}^-$ (0.0 MeV) and $\frac{3}{2}^-$ (1.94 MeV) state, respectively. In Fig. 5 angular distributions for transitions to several states in ^{41}Ca are shown where the solid lines are the result of DWBA calculations which will be discussed in Sec. IV.

The complications in the energy spectra due to ejectile excitations are still more severe for the reaction ^{40}Ca(^{18}O,^{19}F)^{39}K. As seen in Fig. 4(b) the ground state of ^{39}K is populated with ^{19}F in its $\frac{1}{2}^+$ (g.s.) and $\frac{5}{2}^+$ (0.197 MeV) excited states. From the present experiment no conclusion can be drawn about the strength of the ^{19}F ($\frac{1}{2}^-$) state at $E_x=0.110$ MeV which is expected to be only weakly excited based on the result of the ^{18}O(^{3}He,d)^{19}F reaction.[18] The strength at 1.4 MeV corresponds to the excitation of the $\frac{3}{2}^+$ state in ^{19}F with ^{39}K in its ground state. The group at 2.5 MeV excitation energy is again interpreted as a multiplet with ^{19}F in its $\frac{1}{2}^+$ and $\frac{5}{2}^+$ states and ^{39}K in its $\frac{1}{2}^+$ excited

TABLE I. Optical model potential parameters used in the DWBA and coupled channel calculations for $^{18}O+^{40}Ca$ at $E_{lab}=62.14$ MeV.

	$-V_0$ (MeV)	r_0 (fm)	a (fm)	$-W$ (MeV)	r_0' (fm)	a' (fm)
DWBA	14.4	1.374	0.521	7.6	1.381	0.518
CC	14.4	1.374	0.521	6.35	1.267	0.60

state. Owing to the uncertainties in identifying discrete states no angular distributions were extracted. An estimate of the overall, angle-integrated transition strength to low-lying ($E_x<6$ MeV) states in the $^{19}F+^{39}K$ final channels yields a value of 10–15% of the strength of the corresponding $^{17}O+^{41}Ca$ final channels.

IV. DISCUSSION

A. Elastic scattering

Optical potential parameters for the DWBA and CC calculations were obtained by performing least squares fits to the elastic scattering angular distribution. As start parameters the different potential families obtained[22] in the analysis of ^{16}O scattering on ^{48}Ca at $E_{lab}=56$ MeV were used. In each family the potential parameters obtained differ only slightly from the ^{16}O results, mainly showing an increase of the real potential by about 2–3%. It was shown in Ref. 23 that angular distributions for inelastic scattering measured at energies in the vicinity of the Coulomb barrier ($E/E_C<2$) do not provide additional constraints on the choice of the optical potential. Therefore, the same type of potential as used previously for the $^{16}O+^{40}Ca$ system[3] was chosen for the DWBA and CC calculations (see Table I).

B. DWBA analyses for inelastic scattering and transfer reactions

1. Projectile excitation

The angular distribution for excitation of the 2^+ state in ^{18}O at $E_x=1.982$ MeV (see Fig. 3) exhibits a sharp minimum at $\theta_{c.m.}=28°$. Cross sections for angles smaller than $\theta_{c.m.}=22°$ could not be extracted due to the ^{12}C and ^{16}O contaminants in the ^{40}Ca targets. The dashed line in Fig. 4 is the result of a DWBA calculation with the code PTOLEMY.[19] The $B(E2)$ value was taken from the literature[8] and the same mass and charge deformation length was used in the calculation (see Table II). A shift of the theoretical angular distribution towards larger angles by about 3° is observed. In addition, the cross section at $\theta_{c.m.}=40°$ is underpredicted by about 50%. This can be remedied by choosing a larger value for the mass deformation parameters β_N, as was done, for example, in the analysis of ^{18}O inelastic scattering on $^{58,64}Ni$ (Ref. 10). The 65% *ad hoc* change in β_N ($^{18}O^{2+}$), however, can only be partially justified by results of $\pi^{\pm}$ inelastic scattering.[24] On the other hand, recent coupled-channels calculations for $^{18}O+^{40}Ca$ were capable of reproducing the ^{18}O (2^+) data through the microscopic treatment of the form factor, without an *ad hoc* change in the β_N value. This is described in detail in Ref. 25 (see Fig. 7 therein). We have, therefore, made no further attempt to improve the description between data and CC calculation by a change in β_N.

A disagreement between experiment and DWBA description is also observed for the inelastic excitation of the ^{18}O (3^-) state at $E_x=5.098$ MeV in ^{18}O. Taking the $B(E3)$ value from inelastic electron scattering[36] and assuming equal deformation length for mass and charge deformation, the dotted line in Fig. 3 is obtained which underpredicts the cross section at $\theta_{c.m.}=40°$ by a factor of 2. This also may be

TABLE II. Deformation lengths for transitions in ^{18}O and ^{40}Ca used in the DWBA and CC calculations.

Nucleus	J_i^{π}	J_f^{π}	Transition energy (MeV)	δ_c (fm)	δ_N DWBA (fm)	δ_N CC (fm)
^{18}O	0^+	2^+	1.982	1.00	1.00	1.00
^{18}O	0^+	3^-	5.098	0.62	0.80	0.68
^{40}Ca	0^+	3^-	3.737	1.79	1.08	1.02
^{40}Ca	0^+	2^+	3.905	0.47	0.41	0.41
^{40}Ca	0^+	5^-	4.492	1.22	0.54	0.38
^{40}Ca	3^-	5^-	0.755	0.27		0.19

TABLE III. Spectroscopic factors for several low-lying states in ^{41}Ca obtained from the present DWBA calculations in comparison with the results from other work.

State ^{41}Ca	State ^{17}O	E^* (MeV)	$S_1S_2(^{18}O,^{17}O)$ Present work	$S_1S_2(^{18}O,^{17}O)$ $E_{lab}=50$ MeV[b]	$S_1(d,p)$ $E_{lab}=7$ MeV[c]	$S_1(d,p)$ $E_{lab}=10$ MeV[d]	$S_1(d,p)$ $E_{lab}=11$ MeV[e]	$S_1(d,p)$ $E_{lab}=12$ MeV[f]	S_1^a Present work
$\frac{7}{2}^-$	$\frac{5}{2}^+$	0.0	2.32	1.22	0.8	0.84	0.95	0.89	1.46
$\frac{7}{2}^-$	$\frac{1}{2}^+$	0.871	0.29	0.20	0.8	0.84	0.95	0.89	1.06
$\frac{3}{2}^-$	$\frac{5}{2}^+$	1.943	1.14	1.00	0.65	0.60	0.70	0.68	0.72
$\frac{3}{2}^-$	$\frac{5}{2}^+$	2.462	0.32	0.26	0.22	0.20	0.25	0.22	0.20
$\frac{3}{2}^-$	$\frac{1}{2}^+$	2.814	0.23		0.65	0.60	0.70	0.68	0.86
$\frac{1}{2}^-$	$\frac{5}{2}^+$	3.944	0.73	0.65	0.60	0.50	0.65	0.55	0.46

[a]Assuming (^{18}O,^{17}O) spectroscopic factors $S_2(d_{5/2})=1.59$ and $S_2(s_{1/2})=0.27$ (Ref. 29).
[b]Reference 27.
[c]Reference 20.
[d]Reference 31.
[e]Reference 21.
[f]Reference 32.

related to the fact that a microscopic form factor was not used in the DWBA calculation.

2. Target excitation

The angular distributions for excitation of the 3^-, 2^+, and 5^- states in ^{40}Ca are shown in Fig. 3. While the angular distribution of the ^{40}Ca (3^-) state at $E_x=3.737$ MeV is not significantly disturbed by an unresolved contribution from projectile excitation, the angular distributions for the transitions to the 2^+ and 5^- states in ^{40}Ca may contain some contributions from excitation of the ^{18}O (2^+) and ^{18}O (1^-) states at $E_x=3.921$ MeV and $E_x=4.456$ MeV, respectively. When compared to the ^{16}O+^{40}Ca system, the angular distribution of the 3^- state does not show as strong a forward peaking. On the other hand, the angular distribution of the 5^- state again shows a rapid falloff at larger angles. The dashed lines in Fig. 3 are DWBA calculations with the code PTOLEMY using the charge and mass deformation lengths given in Table II. While the angular distribution for the 3^- transition is reasonably well described by DWBA theory, the distribution for the 5^- state is poorly reproduced. This behavior is similar to that observed for ^{16}O+^{40}Ca, where it was found that the results can be understood in the framework of CC calculations as being due to the influence of a single strongly-excited channel, i.e., the ^{40}Ca (3^-) state, on the scattering wave functions. In the present case, the dominant transitions are the excitation of the ^{18}O (2^+) state with cross sections exceeding 20 mb/sr and the excitation of the ^{40}Ca (3^-) state with cross sections approaching 10 mb/sr.

3. Transfer reactions

DWBA calculations were performed for the one neutron stripping reaction (^{18}O,^{17}O) using the finite range DWBA code PTOLEMY.[19] The results are shown as solid lines in Fig. 5, where the calculated cross sections were normalized to the angular distributions and spectroscopic factors extracted. The bell shaped form of the measured angular distributions is in general well described. In particular, the angular distribution populating the ^{17}O ($\frac{1}{2}^+$) state leaving ^{41}Ca in its $\frac{7}{2}^-$ ground state is in very good agreement with the data. This behavior is somewhat unexpected because in many other cases ejectile excitation is very poorly described by DWBA.[27,28] The experimental angular distribu-

tions populating excited states in ^{41}Ca with ^{17}O in its $\frac{5}{2}^+$ ground state show smaller widths than the one observed for ejectile excitation. Furthermore, the maxima of the angular distributions remain at $\theta_{c.m.} \cong 31°$, independent of the excitation energy. Because the bell shaped angular distributions calculated within the DWBA predict the same widths for all cases with maxima shifting to larger angles with increasing excitation energy, the agreement between experiment and theory becomes worse for states in ^{41}Ca with higher excitation energies. The products of the spectroscopic factors extracted from the experimental data are shown in the third column of Table III. In order to obtain the spectroscopic factors for the states in ^{41}Ca, the (^{18}O,^{17}O) spectroscopic factors were taken as 1.59 ($d_{3/2}$) and 0.27 ($s_{1/2}$) (see Ref. 29). As can be seen from Table III, our results are in good agreement with an earlier measurement of the ^{40}Ca(^{18}O,^{17}O)^{41}Ca reaction at 50 MeV incident energy,[27] with the exception of the ^{41}Ca ($\frac{7}{2}^-$) g.s. transition which shows a spectroscopic factor of 1.46 in the present experiment. It would be interesting to investigate if two-step processes with inelastic scattering as an intermediate channel can explain the large spectroscopic factor observed for the ^{40}Ca(^{18}O,^{17}O)^{41}Ca ($\frac{7}{2}^-$ 0.0) reaction.

C. Coupled channel calculations for inelastic scattering

It was shown in Ref. 3 that due to the strong contribution from the inelastic transition to the ^{40}Ca (3^-) state in the ^{16}O+^{40}Ca reaction, conventional DWBA calculations are not able to describe the measured inelastic angular distributions; in particular for transitions with high multipolarity, an explicit treatment of the effect of the 3^- transition on the elastic scattering wave function was necessary in the framework of a CC calculation. (Another approach has been shown to successfully describe the data by performing a single-step DWBA calculation for the inelastic excitation of the 5^- state, but still using an optical model potential derived in a CC calculation.[4]) The system ^{18}O+^{40}Ca differs from the reaction ^{16}O+^{40}Ca in that many more channels [e.g. (^{18}O,^{17}O), (^{18}O,^{16}O), and (^{18}O,^{18}O*)] compete for the available flux and it could be possible that a DWBA treatment, where the effects of various channels are contained in the imaginary part of the optical potential, may be more justified, similar to the ^{11}B+^{40}Ca system studied recently.[30] From a comparison of the data with the DWBA calculations (dashed lines in Fig. 3), it is observed that with the exception of the 5^- transition the angular distributions for the target excitation are reasonably well reproduced. In order to see if a coupled channel treatment can improve the agreement, we have performed calculations along similar lines as in Ref. 3 using the program PTOLEMY. The coupling scheme is indicated in Fig. 6 and the results are shown as solid lines in Fig. 3. The parameters used in these calculations are given in Tables I and II. The imaginary part of the optical potential was modified so as to reproduce elastic scattering in a coupled channel calculation including the ground state, ^{40}Ca (3^-) and ^{18}O (2^+) state. As starting values the results[3] for ^{16}O+^{40}Ca were used. The CC results show a slightly improved agreement with the experimental data over the DWBA calculations; in particular the slopes of the angular distributions for the ^{40}Ca (5^-) and ^{18}O (3^-) states are increased, which is in agreement with the experimental data. The results indicate that transitions with high multipolarity are particularly sensitive to coupled channel effects in the elastic scattering wave functions.

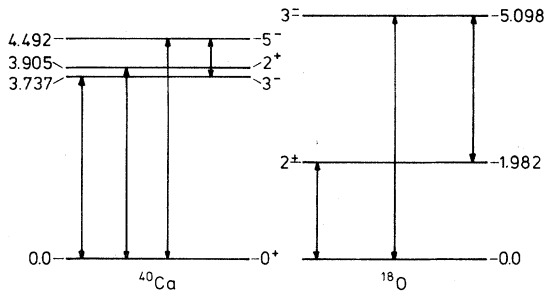

FIG. 6. Coupling scheme used in the CC calculations.

V. SUMMARY

Inelastic scattering of oxygen isotopes on ^{40}Ca has revealed some interesting features which connect the conventional DWBA calculations with the more complex CC approach. Transitions with, in particular, high multipolarity ($L = 5$ and to a lesser extent $L = 3$) seem to be sensitive to details of the scattering wave functions. The results for the ^{16}O+^{40}Ca system, in which there are only a few important reaction channels, indicated that the usual prescription to account for all channels, not treated explicitly, by the imaginary part of the entrance channel optical potential is not justified. The present ^{18}O+^{40}Ca results indicate that with increasing number of open channels the effect weakens and

DWBA gives a better description of the data. It would be interesting to study the energy dependence of this effect for the system $^{16}O+^{40}Ca$, since the number of open channels will increase with energy. For the excitation of the ^{18}O (2^+) state the same discrepancies as already found in earlier studies are observed. The theoretical angular distribution is shifted to larger angles and the cross sections at large angles are underpredicted by about a factor of 2 if standard values for β_N are used. This discrepancy most likely is related to the fact that no microscopic form factor was used in the calculations.[25] The experimental results obtained for the $(^{18}O,^{17}O)$ one neutron transfer reaction are in quite good agreement with the DWBA calculations when spectroscopic factors from light ion induced reactions are used.

ACKNOWLEDGMENTS

One of us (K.E.R.) gratefully acknowledges the support by a Fellowship from the Max Kade Foundation during this work. This research was performed under the auspices of the U.S. Department of Energy under Contract W-31-109-Eng-38.

*Present address: U.S. Department of Energy, Washington, D.C. 20545.

[1]D. L. Hillis, E. E. Gross, D. C. Hensley, L. D. Rickertsen, C. R. Bingham, A. Scott, and F. T. Baker, Phys. Rev. Lett. 36, 304 (1976); D. L. Hillis, E. E. Gross, D. C. Hensley, C. R. Bingham, F. T. Baker, and A. Scott, Phys. Rev. C 16, 1467 (1977).

[2]B. Kim, Phys. Lett. 80B, 353 (1979).

[3]K. E. Rehm, W. Henning, J. R. Erskine, and D. G. Kovar, Phys. Rev. Lett. 40, 1479 (1978).

[4]R. J. Ascuitto, J. F. Petersen, and E. A. Seglie, Phys. Rev. Lett. 41, 1159 (1978).

[5]E. E. Gross, T. P. Cleary, J. L. C. Ford, D. C. Hensley, and K. S. Toth, Phys. Rev. C 17, 1665 (1978).

[6]Nyguyen Van Sen, G. Ratel, R. Darves-Blank, J. C. Gondrand, and F. Merchez, Phys. Rev. C 17, 639 (1978).

[7]K. E. Rehm, H. J. Körner, M. Richter, H. P. Rother, J. P. Schiffer, and H. Spieler, Phys. Rev. C 12, 1945 (1975).

[8]H. Essel, K. E. Rehm, H. Bohn, H. J. Körner, and H. Spieler, Phys. Rev. C 19, 2224 (1979).

[9]J. S. Blair, in *Direct Interactions and Nuclear Reaction Mechanisms,* edited by E. Clementel and C. Villi (Gordon and Breach, New York, 1963), p. 669.

[10]R. A. Broglia, in *Proceedings of the International Conference on Reactions between Complex Nuclei, Tennessee, 1974,* edited by R. L. Robinson, F. M. McGowan, J. B. Ball, and J. H. Hamilton (North-Holland, Amsterdam, 1974), Vol. II, pp. 303–326; F. Videback, P. R. Christensen, O. Hansen, and K. Ulbak, Nucl. Phys. A256, 301 (1976).

[11]A. J. Baltz and S. Kahana, Phys. Rev. C 17, 555 (1978).

[12]K. S. Low, J. Phys. Soc. Jpn., Suppl. 44, 267 (1979).

[13]S. Landowne and H. H. Wolter, Phys. Rev. Lett. 43, 1233 (1979).

[14]S. Landowne, R. Schlicher, H. H. Wolter, K. E. Rehm, E. Müller, I. C. Oelrich, J. Paschopoulos, and H. Rösler, Phys. Lett. 90B, 389 (1980).

[15]J. R. Erskine, T. H. Braid, and J. C. Stoltzfus, Nucl. Instrum. Methods 135, 67 (1976).

[16]R. Vandenbosch, W. N. Reisdorf, and P. H. Lau, Nucl. Phys. A230, 59 (1974).

[17]B. G. Harvey, J. R. Meriwether, J. Mahoney, A. Bussière de Nercy, and D. J. Horen, Phys. Rev. 146, 712 (1966).

[18]F. Ajzenberg-Selove, Nucl. Phys. A300, 1 (1978).

[19]M. H. Macfarlane and S. C. Pieper, Argonne National Laboratory Report No. ANL-76-11-Rev. 1, 1978.

[20]T. A. Belote, A. Sperduto, and W. W. Buechner, Phys. Rev. 139, B80 (1965).

[21]D. C. Kocher and W. Haeberli, Nucl. Phys. A196, 225 (1972).

[22]W. Henning, Y. Eisen, J. R. Erskine, D. G. Kovar, and B. Zeidman, Phys. Rev. C 15, 292 (1977).

[23]K. E. Rehm, W. Henning, J. R. Erskine, D. G. Kovar, M. H. Macfarlane, S. C. Pieper, and M. Rhoades-Brown, Phys. Rev. C 25, 1915 (1982).

[24]S. Iversen, A. Obst, K. K. Seth, H. A. Thiessen, C. L. Morris, N. Tanaka, F. Smith, J. F. Amann, R. Boudrie, G. Burleson, M. Devereux, L. W. Swenson, P. Varghese, K. Boyer, W. J. Braithwaite, W. Cottingame, and C. F. Moore, Phys. Rev. Lett. 40, 17 (1978).

[25]S. Landowne, R. Schlicher, and H. H. Wolter, Nucl. Phys. A373, 141 (1982).

[26]J. L. Groh, R. P. Singhal, H. S. Caplan, and B. S. Dolbilkin, Can. J. Phys. 49, 2743 (1971).

[27]J. F. Petersen, D. Dehnhard, and B. F. Bayman, Phys. Rev. C 15, 1719 (1977).

[28]D. G. Kovar, W. Henning, B. Zeidman, Y. Eisen, J. R. Erskine, H. T. Fortune, T. R. Ophel, P. Sperr, and S. E. Vigdor, Phys. Rev. C 17, 83 (1978).

[29]R. D. Lawson, *Theory of the Nuclear Shell Model* (Oxford University, London, 1980).

[30]V. Hnizdo, C. W. Glover, and K. W. Kemper, Phys. Rev. C 23, 236 (1981).

[31]G. Brown, A. Denning, and J. G. B. Haigh, Nucl. Phys. A225, 267 (1974).

[32]O. Hansen, J. R. Lien, O. Nathan, A. Sperduto, and P. O. Tjom, Nucl. Phys. A243, 100 (1975).